DNA Nanomachines

International Edition: DOI: 10.1002/anie.201506312
German Edition: DOI: 10.1002/ange.201506312

Binding-Induced DNA Nanomachines Triggered by Proteins and Nucleic Acids

Hongquan Zhang, Maode Lai, Albert Zuehlke, Hanyong Peng, Xing-Fang Li, and X. Chris Le**

Abstract: *We introduce the concept and operation of a binding-induced DNA nanomachine that can be activated by proteins and nucleic acids. This new type of nanomachine harnesses specific target binding to trigger assembly of separate DNA components that are otherwise unable to spontaneously assemble. Three-dimensional DNA tracks of high density are constructed on gold nanoparticles functionalized with hundreds of single-stranded oligonucleotides and tens of an affinity ligand. A DNA swing arm, free in solution, is linked to a second affinity ligand. Binding of a target molecule to the two ligands brings the swing arm to AuNP and initiates autonomous, stepwise movement of the swing arm around the AuNP surface. The movement of the swing arm, powered by enzymatic cleavage of conjugated oligonucleotides, cleaves hundreds of oligonucleotides in response to a single binding event. We demonstrate three nanomachines that are specifically activated by streptavidin, platelet-derived growth factor, and the Smallpox gene. Substituting the ligands enables the nanomachine to respond to other molecules. The new nanomachines have several unique and advantageous features over DNA nanomachines that rely on DNA self-assembly.*

Biological or synthetic molecular machines, assembled with molecular components, perform quasi-mechanical movements in response to specific external stimuli.[1] The exquisite specificity, predictability, and diversity of DNA hybridization has inspired the use of DNA to construct various nanomachines, including DNA walkers,[2] DNA tweezers,[3] DNA motors,[4] DNA robots,[5] and DNA switches.[6] These DNA nanomachines are constructed on the basis of DNA self-assembly,[7] usually activated by nucleic acids. The few non-nucleic acid nanomachines require conformation changes of the functional DNA upon molecular interactions.[8] There are very few protein-activated nanomachines.[9]

We report here a new type of DNA nanomachine that is activated by protein binding. Distinct from existing DNA nanomachines that are formed by DNA self-assembly, the new nanomachine is constructed with and activated by binding-induced DNA assembly.[10] The binding of a single target molecule with two ligand molecules triggers the assembly of separate DNA components that are otherwise unable to spontaneously assemble. Taking advantage of the high DNA loading capacity of gold nanoparticles (AuNPs), we constructed a binding-induced nanomachine to possess high density, three-dimensional DNA tracks, representing an advance over the existing one- or two-dimensional DNA nanomachines. Specific target binding triggers autonomous, stepwise movement of a swing arm along the AuNP surface, generating hundreds of oligonucleotides in response to a single binding event. The nanomachine is applicable to any molecules capable of binding simultaneously to two ligands.

We designed the binding-induced DNA nanomachine to consist of a DNA-functionalized AuNP and a swing arm (Scheme 1; Supporting Information, Figure S1 a). The surface of a single AuNP is conjugated to hundreds of single-stranded anchorages and tens of an affinity ligand **L1** (determination of anchorage loading on AuNPs is described in the Supporting Information). Each anchorage is composed of a short sequence **C1** that is attached onto the AuNP by a DNA spacer **S1**. On the free end of **C1**, we conjugated a fluorescent tag (FAM), to enable real-time monitoring of the nanomachine operation. Fluorescence is quenched because of the extremely high efficiency of fluorescence quenching by AuNPs.[11] The swing arm is composed of a sequence **C1*** complementary to **C1**, and a polythymine spacer **S2** serving as a flexible linker between **C1*** and a second ligand **L2**. Varying the number of thymines (**S2**) enables us to create a desired arm length between **C1*** and **L2** (Supporting Information, Table S1).

We designed **C1** and **C1*** to contain only 7 complementary nucleotides so that their hybrid is unstable at ambient temperature. We also designed a DNA blocker, complementary to one segment of **C1*** and another segment of **S2**, to further minimize any target-independent spontaneous hybridization between **C1** and **C1*** (Supporting Information, Figure S1 a). Therefore, when there is no interaction between the swing arm and the AuNP, the nanomachine is inactive. However, binding of the target molecule (such as a protein) to both ligands **L1** and **L2** activates the operation of the nanomachine in the following manner. The binding of **L1** and **L2** to the same target molecule places the swing arm onto the AuNP surface. Consequently, the complementary sequences **C1** and **C1*** are brought into close proximity, allowing for intramolecular binding-induced assembly. The intramolecular interaction dramatically increases the local effective concentrations of **C1** and **C1***, enabling the **C1**:**C1*** hybrid to have a higher stability than that of the hybrid between the blocker

[*] Prof. H. Zhang, A. Zuehlke, Dr. H. Peng, Prof. X.-F. Li, Prof. X. C. Le
Department of Laboratory Medicine and Pathology
University of Alberta
Edmonton, T6G 2G3 (Canada)
E-mail: hongquan@ualberta.ca
xc.le@ualberta.ca
Prof. M. Lai
Department of Pathology
Zhejiang University School of Medicine
Hangzhou, Zhejiang, 310058 (China)

Supporting information for this article is available on the WWW under http://dx.doi.org/10.1002/anie.201506312.

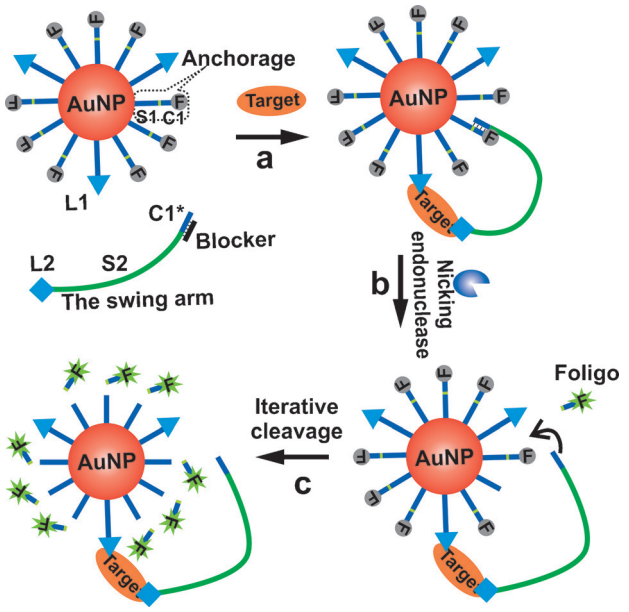

Scheme 1. Binding-induced DNA nanomachine. a) Binding to a target brings the swing arm onto the AuNP surface, inducing the hybridization between **C1*** on the swing arm and **C1** on the anchorage. b) The **C1***:**C1** hybrid has a nicking endonuclease recognition site. The nicking endonuclease cleaves **C1** from the hybrid, leaving single-stranded **C1*** available. The swing arm moves along the AuNP surface, bringing **C1*** to hybridize with **C1** on the next anchorage. c) The iterative operation continues: movement of the swing arm along the AuNP surface, formation of the **C1***:**C1** hybrid, and enzymatic cleavage of **C1** from the hybrid. The cleaved oligonucleotide is fluorescent (Foligo) and is detected. Thus, fluorescence generation serves as a surrogate for monitoring the nanomachine operation. The entire event is initiated by binding of a single target molecule to the two ligands (**L1** and **L2**)

and the swing arm, and driving the formation of a stable hybrid between **C1** and **C1*** by displacing the blocker from the swing arm. The hybridization forms a complete recognition sequence of a nicking endonuclease (NEase; (Supporting Information, Figure S1 b). The NEase-catalyzed cleavage of **C1** from the **C1***:**C1** hybrid liberates **C1***, making it available for hybridization with another **C1** on the same AuNP. Thus, the enzymatic cleavage drives the swing arm to move autonomously along the AuNP surface until all cleavages are complete and the nanomachine stops.

The NEase-catalyzed cleavage of **C1** releases the fluorescently-labeled oligonucleotide (Foligo) from the AuNP. The free Foligos in solution are not quenched by AuNP and become fluorescent. As the swing arm moves around the AuNP and cleaves off **C1**, the nanomachine generates increasing fluorescence. Therefore, we are able to monitor the nanomachine operation in real-time by detecting the fluorescence of the released Foligos.

In principle, altering the ligand molecules enables the nanomachine to be specifically responsive to any target molecules (for example, proteins and nucleic acids) that can be bound simultaneously by two ligand molecules. We describe here three examples of nanomachines that are activated by biotin binding to streptavidin, aptamer binding to platelet-derived growth factor (PDGF), and hybridization to the Smallpox gene.

To test the feasibility of our method, we first constructed a DNA nanomachine that is triggered by binding of two biotin molecules to a streptavidin molecule. One biotin molecule, serving as ligand **L1**, is attached to the AuNP. The second biotin, serving as ligand **L2**, is conjugated to the swing arm (Figure 1 a). In the absence of streptavidin, the swing arm and

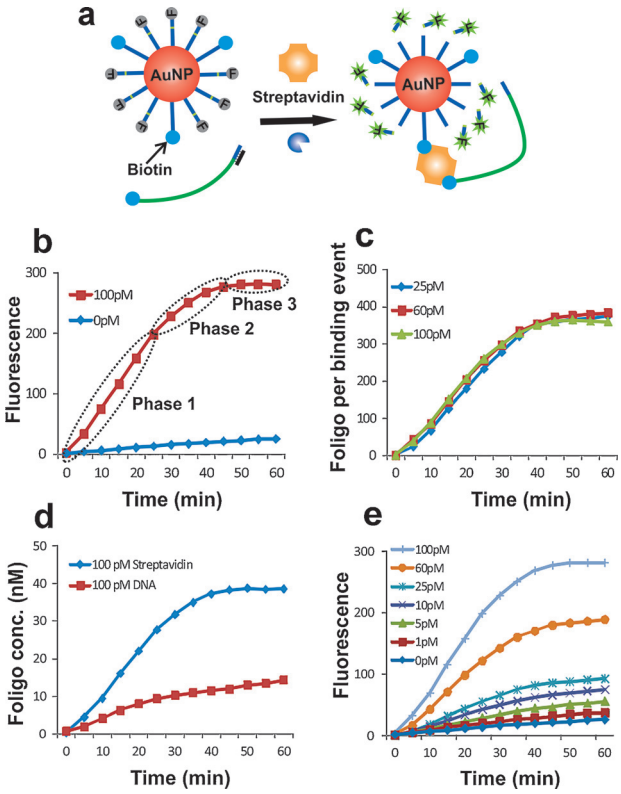

Figure 1. a) Binding of streptavidin to two biotin molecules brings the swing arm to AuNP and leads to enzymatic cleavage of anchorage from AuNP. b) Typical progress curve indicating three phases of the nanomachine operation. c) Number of Foligo generated from a single streptavidin molecule. d) Comparison of anchorage cleavage induced by 100 pM streptavidin and 100 pM control oligonucleotide. e) Response of the nanomachine to various concentrations of streptavidin.

the AuNP exist separately in the solution, and the nanomachine is non-operational. Upon the addition of 100 pM streptavidin to the solution, binding of streptavidin to two biotin molecules (**L1** and **L2**) brings the swing arm into close proximity with the anchorage on the AuNP, activating the nanomachine. Enzymatic cleavage of anchorage from AuNPs gives rise to fluorescence (Figure 1 b). The progress curve reveals that the nanomachine operates in three phases. Once activated, the nanomachine generates Foligo at an initial linear rate for about 25 min (phase 1). Streptavidin binding positions the swing arm in close proximity to anchorages on the AuNP. The enzymatic cleavage follows steady-state kinetics. After a large fraction of anchorages is cleaved off from the AuNP, fewer anchorages with **C1** are available for

hybridization to **C1*** and the nanomachine operation becomes slower (phase 2). Finally, when no **C1** on anchorages is accessible by **C1*** of the swing arm, the operation of nanomachine completes and the fluorescence plateaus (phase 3).

We then tested the efficiency of the nanomachine by monitoring the number of the NEase-cleaved Foligos, originating from a single streptavidin binding, and the subsequent operation of the nanomachine. To ensure that only a single streptavidin molecule is available to bind onto an AuNP, we used a limiting amount of streptavidin and an excess of AuNP. We prepared three solutions containing 200 pM AuNP and 100 pM, 60 pM, or 25 pM streptavidin. Thus, in all three cases, only a single streptavidin molecule could be present on each activated nanomachine. This is supported by TEM and UV/Vis analyses, showing no AuNP aggregation (Supporting Information, Figure S2). The progress curves (Supporting Information, Figure S3) show the time-dependent increases of the overall fluorescence intensity. These results are expected from the operation of the nanomachines. The overall fluorescence intensity is proportional to the total concentration of streptavidin (25, 60, and 100 pM) because a higher concentration of streptavidin in the solution activates more nanomachines, and therefore cleaves off more Foligos. By calibrating the fluorescence intensity against a standard of fluorescent oligo, and knowing the concentrations of streptavidin and AuNP, we have determined the number of Foligos generated from a single nanomachine (activated by a single binding event). The number of Foligos cleaved off from each nanomachine follows a similar profile (Figure 1c). These results suggest that individual nanomachines operate similarly in response to a single binding event. This is understandable because under the conditions of limiting streptavidin concentration, each streptavidin molecule activates a nanomachine by uniting the swing arm and the AuNP, and each activated nanomachine operates independently. Each nanomachine converts a single streptavidin binding event into the cleavage of ~375 Foligos from a single AuNP (Figure 1c). We used 20 nm AuNP and conjugated an average of ~410 anchorages (containing Foligos) onto each AuNP. These results indicate that ~91% of the total Foligos on the AuNP were cleaved off in response to a single binding event, suggesting that our nanomachine is highly efficient.

We compared the performances of three nanomachines that were constructed to have varying lengths of swing arms (40, 60, or 80 n.t.). Similar progress curves from the operation of these three nanomachines (Supporting Information, Figure S4) indicate that these swing arms provide sufficient spatial distance to reach most anchorages on the AuNP. Estimations of the overall size of the loop after the binding-induced formation of the **C1***:**C1** hybrid support these results (Supporting Information, Figure S1b).

We reasoned that the enzymatic cleavage within the nanomachine occurs at a fast rate because of the binding-induced formation of intramolecular hybridization between **C1*** and **C1**. To prove it, we compared the anchorage cleavage from the nanomachine that is triggered by 100 pM streptavidin (Supporting Information, Figure S5a) with the anchorage cleavage from the spontaneous hybridization to 100 pM control oligonucleotide (Supporting Information, Figure S5b). The initial rate of streptavidin-induced nanomachine cleavage is 1.11 $nM^{-1}min^{-1}$, which is significantly larger than that of the DNA-induced cleavage (0.38 $nM^{-1}min^{-1}$; Figure 1d). The higher cleavage rate enables the nanomachine operation to be completed within a short time. Furthermore, in response to a single streptavidin binding, each active nanomachine entity operates with a similar initial rate that is independent of streptavidin concentration (Figure 1c).

The nanomachine can be modulated by varying several parameters. We observed that the number of Foligos generated from a single binding event is proportional to the number of anchorages loaded onto each AuNP (Supporting Information, Figure S6). Thus, altering the anchorage loading amount can manipulate the nanomachine to release desirable oligonucleotides in response to a single molecule binding. Furthermore, we are able to use blockers to reduce target-independent hybridization between **C1** and **C1*** and tune the initial rate of the nanomachine. Increasing the blocker length reduces the initial rate (Supporting Information, Figure S7). Because nucleotides have varying binding affinity to the AuNP surface ($A > C \geq G > T$),[11] varying the spacer **S1** sequence can alter the interaction of the anchorage with AuNP, thereby impacting hybridization of **C1*** with **C1** and the initial rate of the operation (Supporting Information, Figure S8).

Having observed that each active nanomachine operates with a similar progress profile, we reasoned that the total free Foligo in solution is the sum of Foligo cleaved from individual nanomachines and therefore is proportional to the streptavidin concentration. To test this, we measured progress curves resulting from various concentrations of streptavidin (Figure 1e). As expected, the overall fluorescence is proportional to the concentration of streptavidin. The fluorescence intensity at three representative time points is linearly related to the concentration of streptavidin (Supporting Information, Figure S9). The initial rate is also proportional to the streptavidin concentration (Supporting Information, Figure S10). The nanomachine is able to differentiate 0.5 pM streptavidin from the blank. Therefore the nanomachine can be used for sensitive detection of biomolecules, which is conducted in homogeneous solutions, without the need for separation.

We further demonstrate that a simple alteration of affinity ligands enables the nanomachine to be responsive to any other biomolecules that can bind simultaneously to two ligands. As an example, we first used aptamers as affinity ligands to construct a nanomachine specifically responding to PDGF-BB. Because PDGF-BB is a homodimer, containing two identical B chains, we use one aptamer to act as both ligands **L1** and **L2**. The binding of PDGF-BB to both aptamers, one on the AuNP and the second on the swing arm, turns on the nanomachine operation, initiating autonomous and iterative cleavage of the anchorage (Figure 2a). A linear relationship was obtained between PDGF-BB concentration and fluorescence of the cleaved Foligo (Figure 2b). PDGF-BB at 5 pM resulted in a fluorescence increase significantly different from background. The nanomachine

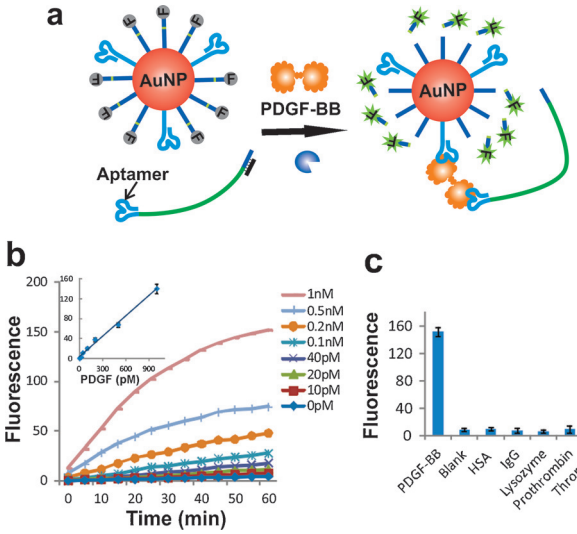

Figure 2. a) Schematic of the nanomachine responsive to PDGF-BB. b) Progress curves of the nanomachine in response to various concentrations of PDGF-BB. Inset: concentration-dependent fluorescence. (c) Specific response of the nanomachine to the target molecule.

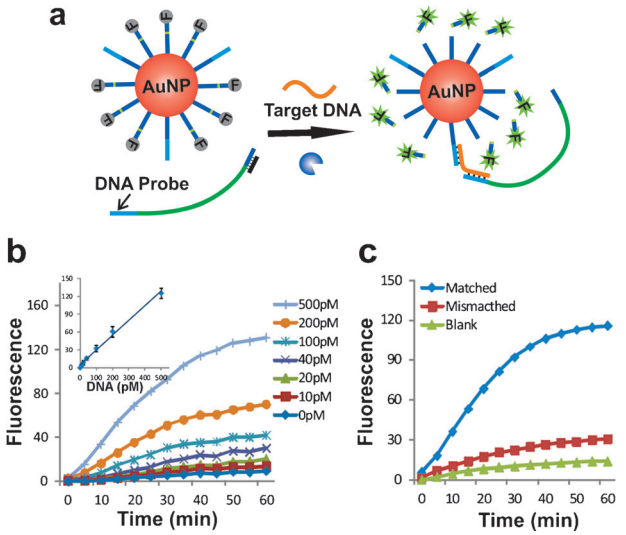

Figure 3. a) Schematic of the nanomachine responsive to the Smallpox gene. b) Progress curves of the nanomachine in response to various concentrations of the Smallpox gene. Inset: concentration-dependent fluorescence. (c) Differentiation of the fully matched target from a single-mismatch.

for PDGF-BB showed lower Foligo generation efficiency than the streptavidin-responsive nanomachine. This is mainly because of the lower binding affinity of PDGF-aptamers compared to streptavidin-biotin binding. We further examined the specificity of the nanomachine by measuring its response to five other proteins (human serum albumin (HSA), human immunoglobulin (IgG), lysozyme, prothrombin, and thrombin). These five proteins at 10 nM concentration did not generate fluorescence distinguishable from the blank, whereas 1 nM PDGF-BB resulted in a large fluorescence increase (Figure 2c). These results suggest that our nanomachine is specifically responsive to the target. The high specificity of the nanomachine largely arises from its distinct feature that activation of the nanomachine necessitates the simultaneous binding of two ligand molecules to the same target molecule. Similar progress curves were obtained when PDGF-BB was present in the cell lysate, further proving the specificity of the nanomachine (Supporting Information, Figure S11).

We further demonstrated the use of DNA probes as affinity ligands to construct a nanomachine specifically responding to a DNA target. We used two DNA probes that enable sandwich hybridization with the Smallpox gene. The Smallpox detection sequence is from the Variola major virus strain Bangladesh-1975. [13] We conjugated one of these probes to the AuNP and incorporated the other probe into the swing arm. The hybridization of a target sequence with two DNA probes brings the swing arm onto the AuNP surface, thereby activating the nanomachine and initiating the generation of Foligos (Figure 3a). The nanomachine operates as expected with a linear relationship between target concentration and fluorescence intensity (Figure 3b). The nanomachine is able to differentiate the fully matched target from a variant of single-mismatch (Figure 3c). The construction of the nanomachine specifically responsive to a DNA target further demonstrates the applicability of nanomachines to various biomolecules.

Distinct from other DNA nanomachines that all rely on DNA self-assembly, the new nanomachines have several advantageous features: i) the binding-induced DNA nanomachines harness specific target binding to trigger assembly of separate DNA components that are otherwise unable to spontaneously assemble. This strategy provides the opportunity to initiate a nanomachine by any target molecule that binds simultaneously to two ligands. (ii) This nanomachine achieves high density, three-dimensional DNA tracks on AuNPs. Other DNA nanomachines are mostly one- or two-dimensional. (iii) The operation of the nanomachine, powered by enzymatic cleavage of conjugated oligonucleotides, cleaves hundreds of oligonucleotides in response to a single binding event, enhancing the sensitivity. The concept and strategy have potential to further expand the dynamic DNA nanotechnology to proteins for diverse applications, such as regulating cell functions, delivering therapeutic drugs, and enhancing molecular imaging.

Acknowledgements

We thank the Natural Sciences and Engineering Research Council of Canada, the Canadian Institutes of Health Research, the Canada Research Chairs Program, Alberta Innovates, Alberta Health, and the 111 Project of China (B13026) for their financial support.

Keywords: DNA assembly · DNA nanomachines · gold nanoparticles · proteins

How to cite: *Angew. Chem. Int. Ed.* **2015**, *54*, 14326–14330
Angew. Chem. **2015**, *127*, 14534–14538

[1] a) P. Karagiannis, Y. Ishii, T. Yanagida, *Chem. Rev.* **2014**, *114*, 3318 – 3334; b) W. R. Browne, B. L. Feringa, *Nat. Nanotechnol.* **2006**, *1*, 25 – 35.

[2] a) P. Yin, H. Yan, X. G. Daniell, A. J. Turberfield, J. H. Reif, *Angew. Chem. Int. Ed.* **2004**, *43*, 4906 – 4911; *Angew. Chem.* **2004**, *116*, 5014 – 5019; b) R. A. Muscat, J. Bath, A. J. Turberfield, *Small* **2012**, *8*, 3593 – 3597; c) Y. Tian, Y. He, Y. Chen, P. Yin, C. Mao, *Angew. Chem. Int. Ed.* **2005**, *44*, 4355 – 4358; *Angew. Chem.* **2005**, *117*, 4429 – 4432.

[3] a) B. Yurke, A. J. Turberfield, A. P. Mills, F. C. Simmel, J. L. Nemann, *Nature* **2000**, *406*, 605 – 608; b) M. Liu, J. Fu, C. Hejesen, Y. Yang, N. W. Woodbury, K. Gothelf, Y. Liu, H. Yan, *Nat. Commun.* **2013**, *4*, 2127; c) C. Zhou, Z. Yang, D. Liu, *J. Am. Chem. Soc.* **2012**, *134*, 1416 – 1418.

[4] a) T. G. Cha, J. Pan, H. Chen, J. Salgado, X. Li, C. Mao, J. H. Choi, *Nat. Nanotechnol.* **2014**, *9*, 39 – 43; b) S. Venkataraman, R. M. Dirks, P. W. Rothemund, E. Winfree, N. A. Pierce, *Nat. Nanotechnol.* **2007**, *2*, 490 – 494; c) M. Liber, T. E. Tomov, R. Tsukanov, Y. Berger, E. Nir, *Small* **2015**, *11*, 568 – 575.

[5] a) Y. Amir, E. Ben-Ishay, D. Levner, S. Ittah, A. Abu-Horowitz, I. Bachelet, *Nat. Nanotechnol.* **2014**, *9*, 353 – 357; b) K. Lund, et al., *Nature* **2010**, *465*, 206 – 210.

[6] a) J. M. Thomas, H. Z. Yu, D. Sen, *J. Am. Chem. Soc.* **2012**, *134*, 13738 – 13748; b) Y. Yang, G. Liu, H. Liu, D. Li, C. Fan, D. Liu, *Nano Lett.* **2010**, *10*, 1393 – 1397; c) F. Wang, X. Liu, I. Willner, *Angew. Chem. Int. Ed.* **2015**, *54*, 1098 – 1129; *Angew. Chem.* **2015**, *127*, 1112 – 1144.

[7] a) J. Bath, A. J. Turberfield, *Nat. Nanotechnol.* **2007**, *2*, 275 – 284; b) H. Liu, D. Liu, *Chem. Commun.* **2009**, 2625 – 2636.

[8] a) C. Song, Z. G. Wang, B. Ding, *Small* **2013**, *9*, 2382 – 2392; b) Z. G. Wang, J. Elbaz, I. Willner, *Nano Lett.* **2011**, *11*, 304 – 309; c) A. Rajendran, M. Endo, K. Hidaka, H. Sugiyama, *J. Am. Chem. Soc.* **2013**, *135*, 1117 – 1123.

[9] S. M. Douglas, I. Bachelet, G. M. Church, *Science* **2012**, *335*, 831 – 834.

[10] a) H. Zhang, X.-F. Li, X. C. Le, *Anal. Chem.* **2012**, *84*, 877 – 884; b) H. Zhang, F. Li, B. Dever, C. Wang, X.-F. Li, X. C. Le, *Angew. Chem. Int. Ed.* **2013**, *52*, 10698 – 10705; *Angew. Chem.* **2013**, *125*, 10894 – 10902; c) B. Deng, J. Chen, H. Zhang, *Anal. Chem.* **2014**, *86*, 7009 – 7016.

[11] a) B. Dubertret, M. Calame, A. J. Libchaber, *Nat. Biotechnol.* **2001**, *19*, 365 – 370; b) B. Bhatt, P. J. Huang, N. Dave, J. Liu, *Langmuir* **2011**, *27*, 6132 – 6137; c) P. Wu, K. Hwang, T. Lan, Y. Lu, *J. Am. Chem. Soc.* **2013**, *135*, 5254 – 5257; d) U. Uddayasankar, U. J. Krull, *Anal. Chim. Acta* **2013**, *803*, 113 – 122.

[12] a) J. J. Storhofff, R. Elghanian, C. A. Mirkin, R. L. Letsinger, *Langmuir* **2002**, *18*, 6666 – 6670; b) H. Kimura-Suda, D. Y. Petrovykh, M. J. Tarlov, L. J. Whitman, *J. Am. Chem. Soc.* **2003**, *125*, 9014 – 9015.13. R. F. Massung, L. I. Liu, J. Qi, J. C. Knight, T. E. Yuran, A. R. Kerlavage, J. M. Parsons, J. C. Venter, J. J. Esposito, *Virology* **1994**, *201*, 215 – 240.

Received: July 8, 2015
Revised: August 17, 2015
Published online: October 12, 2015

